Control of Electronic State by Dihedral Angle in θ-type Bis(ethylenedithio)tetraselenafulvalene Salts

Hatsumi Mori,*,† Naoki Sakurai,†,‡ Shoji Tanaka,† Hiroshi Moriyama,‡ Takehiko Mori,§ Hayao Kobayashi,|| and Akiko Kobayashi⊥

International Superconductivity Technology Center, Shinonome Koto-ku Tokyo 135-0062, Japan, Department of Chemistry, Faculty of Science, Toho University, Miyama, Chiba 274-8510, Japan, Department of Organic and Polymeric Materials, Tokyo Institute of Technology, Tokyo 152-8552, Japan, Institute for Molecular Science, Okazaki 444-0867, Japan, and Department of Chemistry, School of Science, The University of Tokyo, Tokyo 113-0035, Japan

Received April 18, 2000. Revised Manuscript Received July 17, 2000

Five θ-type BETS salts [BETS = bis(ethylenedithio)tetraselenafulvalene], θ-$BETS_2RbCo(SCN)_4$, θ-$BETS_2RbZn(SCN)_4$, θ-$BETS_2CsCo(SCN)_4$, θ-$BETS_2CsZn(SCN)_4$, and θ-$BETS_2Ag(CN)_2$, have been newly prepared by the electrocrystallization method. The crystal structure analyses indicate that the former four salts are isostructural to BEDT-TTF analogues. [BEDT-TTF = bis(ethylenedithio)tetrathiafulvalene] However, the metal−insulator transition temperatures of θ-type BETS salts are much lower than those of isostructural BEDT-TTF salts, due to the smaller *U*/*W* (*U*, intramolecular Coulomb repulsion energy; *W*, bandwidth) of Se-atoms-introduced BETS salts. The electronic phase diagram of θ-type BETS salts indicate that the dihedral angles (θ) between BETS columns in the donor sheet control the electronic states; with decreasing dihedral angle (θ), the transverse interaction (*t*) increases, so that the larger bandwidth ($W = 8t$) makes the metal−insulator transition temperatures lower in the BETS salts. This phase diagram is universal for θ-type BETS salts as well as θ-type BEDT-TTF salts.

Introduction

In the process of the extensive study for organic superconductors,[1,2] some common key parameters have been proposed: (1) pseudo-one-, or two-dimensionality, (2) effective $^1/_2$-band filling, and (3) correlation parameter (*U*/*W*; *U* = on-site Coulomb repulsion of the organic molecule, *W* = bandwidth), but the applicability of these parameters has not been entirely explored yet. To study the scope of these criteria, it is of importance to investigate the electronic state in the vicinity of superconducting state. Recently we have studied the electronic state of θ-type BEDT-TTF (= ET) salts, which include nonmagnetic and paramagnetic insulators, one superconductor (θ-ET_2I_3[3]), and metals.[4−8] Our proposed universal phase diagram is represented by the dotted line in Figure 1; this shows that the metal−insulator transition temperatures are controlled by the dihedral angle between donor columns (θ) or equivalently by the bandwidth ($W = 8t$). As the dihedral angle increases, the transfer integral in the transverse direction (*t*), which determines the bandwidth ($W = 8t$), decreases, and then the electronic state changes from metallic, superconducting to paramagnetic and nonmagnetic insulating phases. For θ-$ET_2RbM'(SCN)_4$ [M′= Co, Zn], the metal−insulator transition temperatures in the rapid and slow-cooling runs are different, due to the existence of the lattice modulation. To obtain more stable metals and to investigate the boundary between metallic and insulating phases, we have adopted a BETS molecule, which has the same framework as ET and smaller *U*/*W* due to the introduction of the Se atoms (Figure 1). Recently there have been a few papers that report the change of electronic state by the replacement of the S atoms of ET with the Se atoms of BETS molecules. For the κ-type salts, κ-$ET_2Cu[N(CN)_2]Br$ is a superconductor,[9] whereas κ-$BETS_2Cu[N(CN)_2]Br$ shows metallic behavior down to 2 K.[10] As for α-phase, the metal−insulator transition temperatures decrease from

* To whom correspondence should be addressed: fax +81-3-3536-0618; e-mail mori@istec.or.jp.
† ISTEC.
‡ Toho University.
§ Tokyo Institute of Technology.
|| Institute for Molecular Science.
⊥ The University of Tokyo.

(1) Ishiguro, T.; Yamaji, K.; Saito, G. *Organic Superconductors*; Springer-Verlag: Berlin and Heidelberg, 1998.
(2) Williams, J. M.; Ferraro, J. R.; Thorn, R. J.; Calrson, K. D.; Geiser, U.; Wang, H. H.; Kini, A. M.; Whangbo, M.-H. In *Organic Superconductors (including Fullerenes) Synthesis, Structure, Properties and Theory*; Prentice Hall: Englewood Cliffs, NJ, 1992.
(3) Kobayashi, H.; Kato, R.; Kobayashi, A.; Nishio, Y.; Kajita, K.; Sasaki, W. *Chem. Lett.* **1986**, 789 and 833.
(4) Mori, H.; Tanaka, S.; Mori, T.; Maruyama, Y. *Bull. Chem. Soc. Jpn.* **1995**, *68*, 1136.
(5) Mori, H.; Tanaka, S.; Mori, T. *J. Phys. I (Fr.)* **1996**, *6*, 1987.
(6) Mori, T.; Fuse, A.; Mori, H.; Tanaka, S. *Phys. C* **1996**, *264*, 22.
(7) Mori, H.; Tanaka, S.; Mori, T.; Kobayashi, A.; Kobayashi, H. *Bull. Chem. Soc. Jpn.* **1998**, *71*, 797.
(8) Mori, H.; Tanaka, S.; Mori, T. *Phys. Rev. B* **1998**, *57*, 12023.
(9) Kini, A. M.; Geiser, U.; Wang, H. H.; Carlson, K. D.; Williams, J. M.; Kwok, W. K.; Vandervoort, K. G.; Thompson, J. E.; Stupka, D. L.; Jung, D.; Whangbo, M.-H. *Inorg. Chem.* **1990**, *29*, 2555.

10.1021/cm000321+ CCC: $19.00
Published on Web 09/13/2000

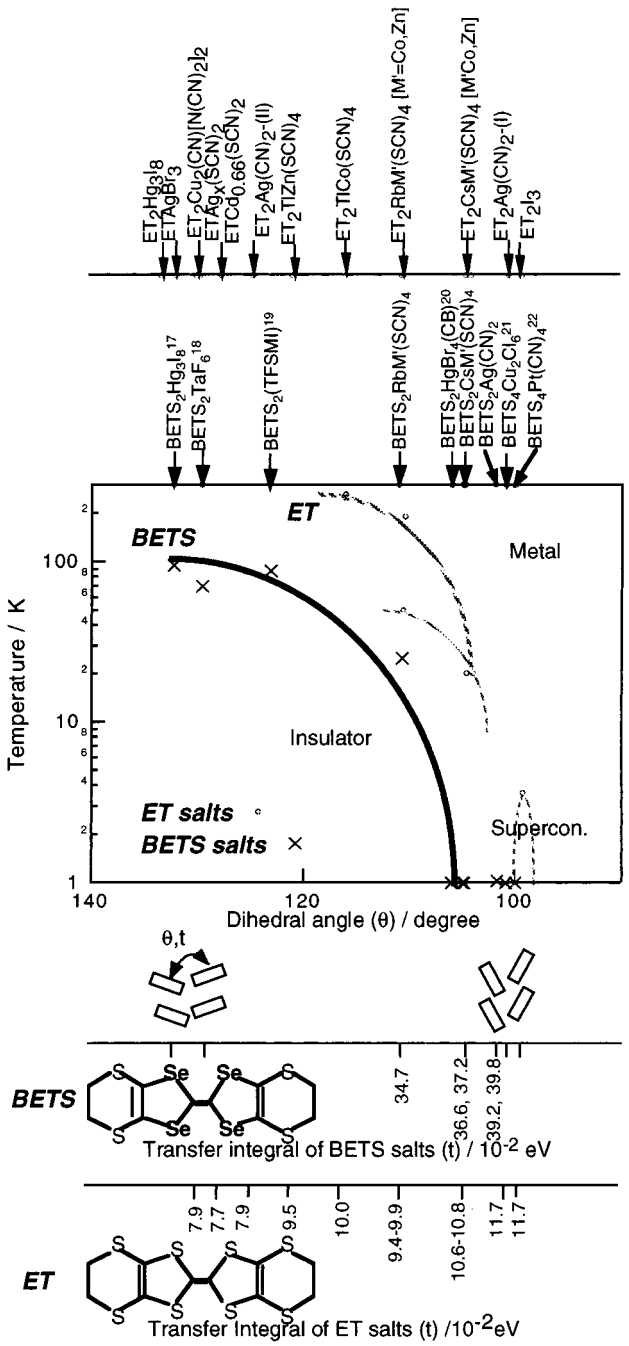

Figure 1. Electronic phase diagram of θ-type ET and BETS salts.

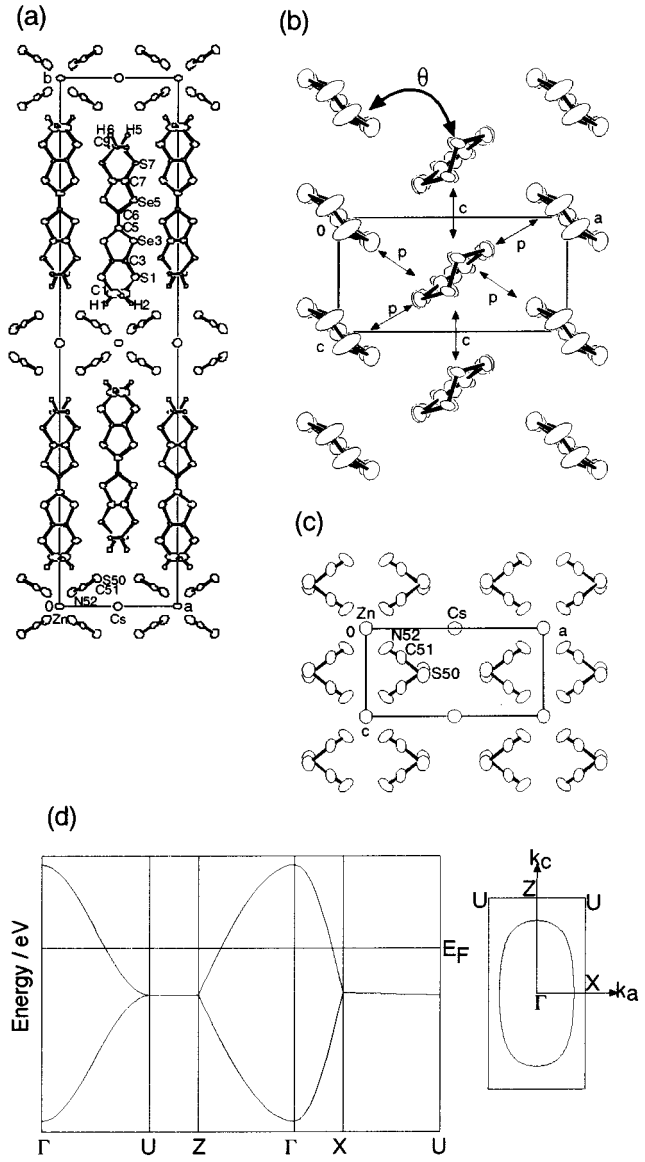

Figure 2. (a) Crystal structure, (b) donor arrangement, (c) anion arrangement, and (d) Fermi surface of θ-$BETS_2CsZn(SCN)_4$.

α-ET_2I_3 (135 K),[11] α-STF_2I_3 (80 K) [STF = bis(ethylenedithio)diselenadithiafulvalene],[12] to α-$BETS_2I_3$ (50 K).[13] However, there is no report in which the effect of the introduction of the Se atoms for θ-phase is discussed. Then, this paper is the first report that shows the systematic study of electronic state for θ-type salts and indicates the effect of the introduction of Se atoms into donor molecules.

Experimental Section

BETS was synthesized by following the previous report.[13] Single crystals of θ-$BETS_2MM'(SCN)_4$ [MM′= RbCo, RbZn, CsCo, or CsZn] and θ-$BETS_2Ag(CN)_2$ were newly prepared by the electrocrystallization of BETS (8 mg) in the presence of MSCN (50 mg), $M'(SCN)_2$ (30 mg) [or $KAg(CN)_2$ (50 mg)], and 18-crown-6 (50 mg) in 1,1,2-trichloroethane (12 mL) containing 10% (v/v) ethanol under N_2.[14] The constant current of 0.5 μA is kept at 20 °C. The obtained crystals were washed with EtOH and air-dried at room temperature.

The electrical resistivity is measured by the conventional four-probe method with application of a low DC current of 10−1000 μA in the range of 300−1.3 K. Gold wires (Tanaka Kikinzoku, 18 μm ϕ) were attached to a crystal with gold paste (Tokuriki Chemicals, no. 8560) as electrodes.

The data were collected on a Rigaku AFC5R diffractometer [Mo−Kα (λ = 0.71073 Å); 50 kV, 150 mA; $2\theta \leq 60°$, $\omega-2\theta$ scan technique) and corrected for the usual Lorentz and polarization

(10) Montgomery, L. K.; Burgin, T.; Huggman, J. C.; Calrson, K. D.; Dudek, J. D.; Yaconi, G. A.; Megnam L. A.; Mobley, P. R.; Kwok, W. K.; Williams, J. M.; Shirber, J. E.; Overmyer, D. L.; Ren, J.; Rofira, C.; Whangbo, M.-H. *Synth. Met.* **1993**, *55−57*, 2090.

(11) Bender, K.; Hennig, I.; Schweitzer, D.; Dietz, K.; Endres, H.; Keller, H. J. *Mol. Cryst. Liq. Cryst.* **1984**, *108*, 359.

(12) Naito T.; Kobayashi H.; Kobayashi, A. *Bull. Chem. Soc. Jpn.* **1997**, *70*, 107.

(13) Kato, R.; Kobayashi, H.; Kobayashi, A. *Synth. Met.* **1991**, *41−43*, 2093.

(14) Mori, H. *Int. J. Mod. Phys. B* **1994**, *8*, 1.

Table 1. Crystal Data and Experimental Details for θ-$BETS_2MM'(SCN)_4$[a] and θ-$BETS_2Ag(CN)_2$

	θ-$BETS_2RbCo(SCN)_4$	θ-$BETS_2RbZn(SCN)_4$	θ-$BETS_2CsCo(SCN)_4$	θ-$BETS_2CsZn(SCN)_4$	θ-$BETS_2Ag(CN)_2$
chemical formula	$C_{24}H_{16}N_4RbCoS_{12}Se_8$	$C_{24}H_{16}N_4RbZnS_{12}Se_8$	$C_{24}H_{16}N_4CsCoS_{12}Se_8$	$C_{24}H_{16}N_4CsZnS_{12}Se_8$	$C_{22}H_{16}N_2S_8Se_8Ag$
formula wt	1521.2	1527.7	1568.7	1575.2	1304.4
system	orthorhombic	orthorhombic	orthorhombic	orthorhombic	monoclinic
space group	*I*222 (23)	*I*222 (23)	*I*222 (23)	*I*222 (23)	C2 (5)
a (Å)	10.128 (9)	10.137 (5)	9.812 (4)	9.818 (6)	10.802 (6)
b (Å)	43.97 (1)	44.006 (4)	44.104 (4)	44.130 (5)	34.644 (6)
c (Å)	4.71 (1)	4.709 (7)	4.907 (5)	4.906 (7)	4.981 (8)
α (deg)	90	90	90	90	90
β (deg)	90	90	90	90	117.44 (5)
γ (deg)	90	90	90	90	90
V (Å^3)	2098 (4)	2100 (3)	2123 (1)	2125 (2)	1654 (3)
Z	2	2	2	2	2
R, R_w	0.080, 0.048	0.086 0.067	0.101, 0.071	0.067, 0.044	0.058, 0.043
D_c (g cm^{-3})	2.41	2.42	2.45	2.46	2.62
total reflections	1815	1746	1825	1826	2564
reflections used	680	262	685	632	923
	$\|I_0\| > 3\sigma\|I_0\|$	$\|I_0\| > 3\sigma\|I_0\|$	$\|I_0\| > 2\sigma\|I_0\|$	$\|I_0\| > 2\sigma\|I_0\|$	$\|I_0\| > 3\sigma\|I_0\|$
$2\theta_{max}$ (deg)	60	60	60	60	60
λ (Å)	0.71073	0.71073	0.71073	0.71073	0.71073

[a] MM′ = RbCo, RbZn, CsCo,or CsZn.

Table 2. Overlap Integrals ($\times 10^{-3}$) of θ-$BETS_2MM'(SCN)_4$[a] and θ-$BETS_2Ag(CN)_2$

overlap integrals	θ-$BETS_2$-RbCo(SCN)$_4$	θ-$BETS_2$-RbZn(SCN)$_4$	θ-$BETS_2$-CsCo(SCN)$_4$	θ-$BETS_2$-CsZn(SCN)$_4$	θ-$BETS_2$-Ag(CN)$_2$
c	7.2	4.6	0.17	1.0	
p	−38.2	−34.7	−36.6	−37.2	
c1					0.1
c2					−3.8
a1					39.2
a2					39.1
p1					39.8
p2					39.8

[a] MM′ = RbCo, RbZn, CsCo, or CsZn.

effects. The data collection conditions are partially listed in Table 1. The crystal structures were solved by a direct method (SHELXS86)[15]. The non-hydrogen atoms were refined anisotropically by a least-squares procedures. Hydrogen atoms were included but not refined. The crystal data are listed in Table 1. The overlap integrals were calculated by the extended Hückel method (Table 2) and the tight binding band calculations were carried out based upon the transfer integrals (*t*) proportional to overlap integrals (*S*): $t = ES$, where *E* is a constant of −10.0 eV.[16]

Results and Discussion

The crystal structure analyses reveal that θ−$BETS_2$-$MM'(SCN)_4$ are isostructural with ET analogues as shown in Figure 2;[4−8] the thick anion sheet and the donor layer stack along the *b*-axis. In the donor layer, donors stack regularly by the herringbone-type arrangement (Figure 2b), whereas in the anion sheet, Zn^{2+} is coordinated by four N atoms of NCS^- and Cs^+ is surrounded by eight S atoms to construct a three-dimensional network (Figure 2c). The large transverse interaction of donors (*p*) affords a two-dimensional Fermi surface (Figure 2d). The unit cell volumes increase by 2.3−2.5% (∼50 Å^3) in comparison with the corresponding ET salts, owing to the increase in the *b*-axis by 1.6% and the *c*-axis by 0.7−1.3%. The *a*-axis is almost constant by −0.4 ∼ +0.1%. The dihedral angles (θ) between BETS columns in the donor sheet are the same as those of ET analogues, 105° for θ-$BETS_2CsM'(SCN)_4$ and 111° for θ-$BETS_2RbM'(SCN)_4$, respectively. On the other hand, θ-$BETS_2Ag(CN)_2$ is not isostructural with the ET analogue (Figure 3); this crystal has a monoclinic symmetry and two halves of BETS molecules (A, B) and a half of $Ag(CN)_2$ are the unique fragments. Two kinds of columns (AAA···) and (BBB···) are arranged alternately in the transverse direction (the *a*-axis), where the dihedral angle (θ) is 102° (Figure 3b). No disorder is observed in the anion. The calculated overlap integrals[16] ($\times 10^{-3}$) in the transverse direction (a = 39.2, p = 39.8) are considerably larger than those in the stacking direction ($c1$ = 0.1, $c2$ = −3.8), then two-dimensional Fermi surface is obtained (Figure 3c). The temperature dependence of electrical resistivity is illustrated in Figure 4. The resistivities at room temperature are 0.1−0.01 Ω cm. As for θ−$BETS_2$-$CsM'(SCN)_4$ [M′ = Co, Zn], the resistivities are almost constant down to low temperatures with small increases below 10 K (Figure 4c,d). Whereas the ET analogues have metal−insulator transitions at 20 K. More metallic behavior is observed for θ-$BETS_2Ag(CN)_2$ (Figure 4e).

(15) Sheldrick, G. H. *Crystallographic Computing 3*; Oxford University Press: Oxford, England, 1985; pp 175−189.
(16) Mori, T.; Kobayashi, A.; Sasaki, Y., Kobayashi, H.; Saito, G.; Inokouchi, H. *Bull. Chem. Soc. Jpn.* **1984**, *57*, 627. The parameters of Slater atomic orbitals [ζ exponent, ionization potential (in electron volts)] are as follows; for Se, 4s (2.112, −20.0 eV), 4p (1.827, −11.0), 4d (1.500, −6.8); for S, 3s (2.112, −20.0), 3p (1.825, −11.0), 3d (1.5, −5.44); for C, 2s (1.625, −21.4), 2p (1.625, −11.4)l; for H, 1s (1.0, −13.6).
(17) Bogdanova, O. A.; Gristenko, V. V.; Dyachenko, O. A.; Zhilyaeva, E. I.; Kobayashi, A.; Kobayashi, H.; Lyubovskaya, R. N.; Lyubovskii, R. B.; Shilov, G. V. *Chem. Lett.* **1997**, 675.
(18) Kato, R.; Kobayashi, A.; Miyamoto, A.; Kobayashi, H. *Chem. Lett.* **1991**, 1045.
(19) Tanaka, Y.; Kobayashi, A.; Kobayashi, H. private communication; TFSMI = bis(trifluoromethanesulfon)imide.
(20) Naito, T.; Miyamoto, A.; Kobayashi, H.; Kato, R.; Kobayashi, A. *Chem. Lett.* **1991**, 1945.
(21) Kobayashi, A.; Sato, A.; Arai, E.; Kobayashi, H.; Faulmann, C.; Kushch, N.; Cassoux, P. *Solid State Commun.* **1997**, *103*, 371.
(22) Kobayashi, H.; Arai, E.; Sato, A.; Naito, T.; Tanaka, H.; Kobayashi, A.; Saito, T.; Cassoux, P. *Synth. Met.* **1997**, *85*, 1595.

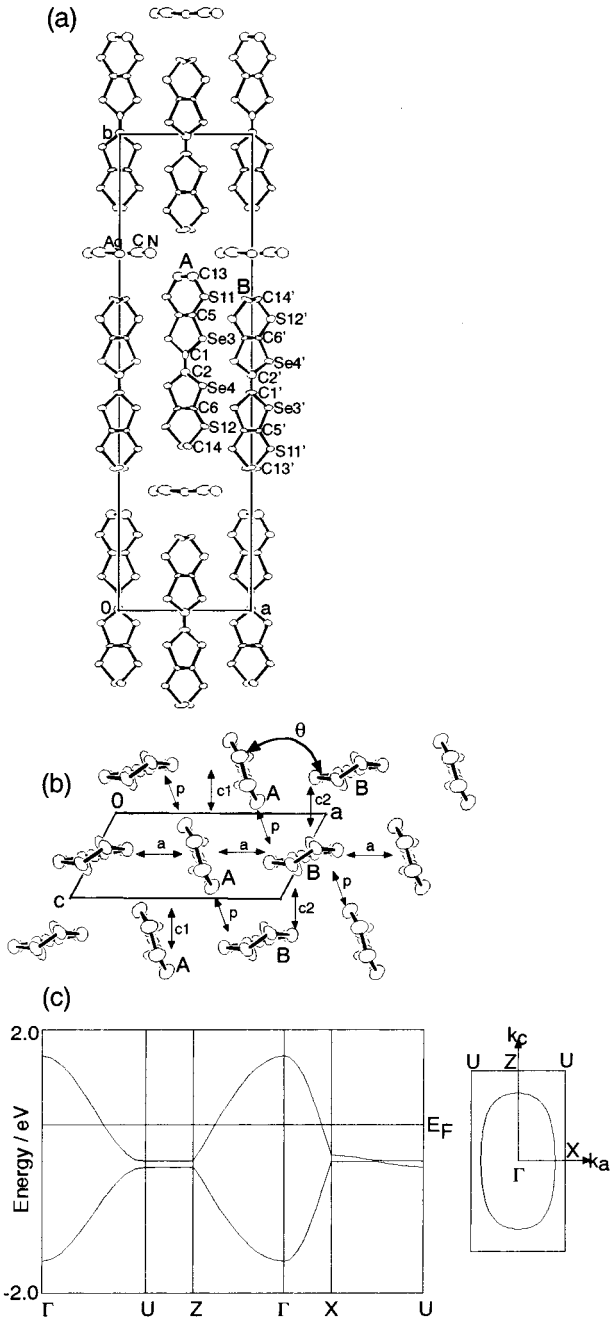

Figure 3. (a) Crystal structure, (b) donor arrangement, and (c) Fermi surface of θ-$BETS_2Ag(CN)_2$.

There is another $[Ag(CN)_2]^-$ salt that shows the metal−insulator transition at 60 K (Figure 4b). A rapid increase of resistivity below 20 K is observed for θ-$BETS_2RbCo(SCN)_4$ (Figure 4a), while the isostructural ET salt has a distinct metal−insulator transition at 190 K with the first-order transition of lattice distortion, where the electron spin resonance (ESR) line width shows a sudden drop.[5] The preliminary ESR measurement for θ-$BETS_2RbCo(SCN)_4$ indicates that the line width at 30 K is around 350 G and decreases monotonically down to 120 G at 5 K without any anomaly, suggesting that the rapid increase of resistivity below 20 K is not the same type of transition as that of the ET analogue.The electronic state of θ-type BETS salts is summarized in the phase diagram in Figure 1, together with θ-type ET salts. All of the transfer integrals (t) of ET and BETS salts are recalculated by using the same parameters based upon the crystal structures, respectively.[16] With the decrease of dihedral angle (θ), the transfer integrals (t) increase systematically. The ET salts [121° ≤ θ, W (= 8t) ≤ 0.80 eV] are the semiconductors at room temperature, [104° ≤ θ ≤ 116°, 0.75 ≤ W ≤ 0.86 eV] show the metal−insulator transitions from 20 to 250 K, and [θ = 99°, W = 0.94 eV] reveals the superconductivity. On the other hands, the BETS salts of θ ≤ 105 ° indicates metallic behaviors down to low temperatures and then, the metal−insulator transition temperatures increase gradually with an increase of θ. Compared with θ-type ET salts, the metallic state of the BETS salts is much more stable and the line of metal−insulator transition temperature seems to be shifted to the left.

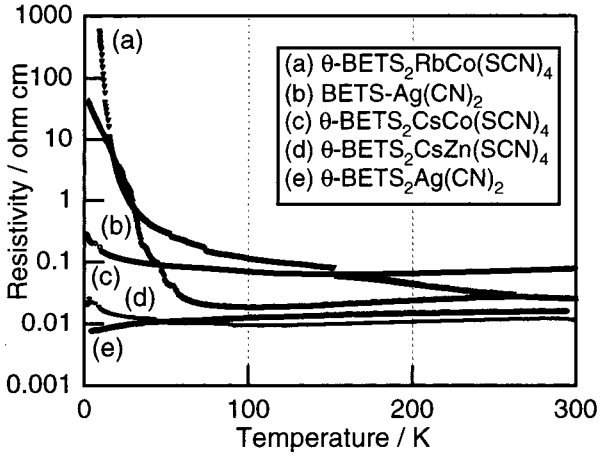

Figure 4. Temperature dependences of electrical resistivity of θ-type BETS salts.

Conclusion

Including the newly prepared θ-type BETS salts, θ-$BETS_2MM'(SCN)_4$ [MM′ = RbCo, RbZn, CsCo, or CsZn] and θ-$BETS_2Ag(CN)_2$, the proposed phase diagram accounts for the electronic state, regulated by the dihedral angle between donor columns (θ) or by the bandwidth (W). Here the metallic state is widely expanded. Now it is clarified that this electronic phase diagram is universal, applicable to BETS salts as well as θ-type ET salts. In other words, the effect of introduction of Se atoms into donor molecules is that the metal−insulator transition temperatures of the θ-type ET salts shift lower systematically with decreasing dihedral angle (θ) or widening the bandwidth (W) in the phase diagram.

Acknowledgment. This work was supported by New Energy and Industrial Technology Development Organization (NEDO).

CM000321+